Organic & Supramolecular Chemistry

Charge Transport in Novel Phenazine Fused Triphenylene Supramolecular Systems

Ashwathanarayana Gowda,[a] Litwin Jacob,[a] Dharmendra P. Singh,[b] Redouane Douali,[b] and Sandeep Kumar*[a]

Novel phenazine–fused triphenylene discotic liquid crystals (DLCs) tethered with alkanethiols and alkoxy chains are synthesized. The condensation of 4,5-dibromobenzene-1,2-diamine with triphenylene-1,2-diquinone discotic core, followed by the reaction with alkanethiols gives heterocyclic phenazine–fused triphenylene based DLCs. The intermediate dibromo–substituted phenazine and final alkanethiol substituted phenazine–fused triphenylene derivatives exhibit a wide range of stable enantiotropic hexagonal columnar phase, which was characterised by polarized optical microscopy (POM), differential scanning calorimetry (DSC) and X-ray diffraction (XRD)

studies. We have also investigated the photophysical properties of all phenazine compounds using dilute solution of anhydrous chloroform. The charge carrier mobility was measured for one representative compound by time of flight method which revealed that phenazine–fused triphenylene discotic mesogen exhibits p-type (hole) mobility of the order of 10^{-4} cm^2 V^{-1} s^{-1}. The novel mesogens reported here present a wide temperature stability with good charge mobility and optical properties. These mesogens have shown potential applications for solar cells, sensors, organic light emitting diodes and other electro-optical device applications.

1. Introduction

The spontaneous self-assembly of appropriately functionalized anisotropic molecules exhibit combined properties of crystalline solid and conventional liquid retaining both the order and mobility at molecular and macroscopic levels.[1] These systems are now termed as liquid crystals (LCs), the intriguing beautiful forth state of matter.[2] The self-healing and self-aligning ability of LCs can be smoothly constructed through weak interactions such as hydrogen bonding, van der Waals forces, $\pi-\pi$ stacking, dipolar or quadrupolar interactions, charge transfer interactions, etc. They have strong impact on daily life device applications.[2–6] In this context, discotic liquid crystals (DLCs) play a vital role in the formation of self-assembled highly ordered columnar phases and hence they have attracted considerable attention owing to their technological applications.[7–13] The general template for designing discotic liquid crystals is essentially consist of a flat, disc-like π-conjugated aromatic core encompassing with an insulating mantle of aliphatic chains. Depending on the molecular interactions, discotic liquid crystals mainly stabilize two general classes of liquid crystalline mesophases. Self-assembly of discotic meso-

gens with orientational order but no long range positional order gives discotic nematic (N$_D$) phase. Discotic nematic phase is less commonly observed but it can acts like an optical compensative film that increases the viewing-angle of liquid crystal displays (LCDs).[6,14–18] Columnar phase formed by one-dimensional anisotropic stacking arrangement of individual π-conjugated disc-like mesogens self-assembled one on top of another to form columns, and the arrangement of these columns in to different lattices defines subclass of mesophases. Thus, large π-orbitals overlap of adjacent conjugated aromatic cores stabilise the columnar phase, supramolecular order and enhance unidirectional charge mobility along the columnar axis.[19–26] The supramolecular self-assembly of columnar structure of DLCs may be considered as quasi-one-dimensional molecular wires, where inherent charge migration occurs in one direction.[2] Owing to their unique electronic and self-healing properties, DLCs have been considered as potential materials for various device applications apart from energy and charge migration. They are extensively applied in organic light emitting diodes (OLEDs),[27–29] organic field effect transistors (OEFT),[30–33] photovoltaic solar cells[22,34,35] and sensors[36,37] etc.

Literature survey reveals that a large number of DLCs derived from triphenylene (TP) exist and they show rich mesomorphism at elevated temperature as well as at ambient temperature.[7] Appropriately functionalised TP derivatives are known for hole-transporting properties and their charge carrier mobility is ranged from 10^{-5} cm^2 V^{-1} s^{-1} to 10^{-1} cm^2 V^{-1} s^{-1} in the highly ordered columnar phase.[38,39] The electron rich nature of TP derivatives are typically known as hole transport materials and are suitable for doping with electron acceptors to serve as a p-type semiconductor. Extension of triphenylene discotic core leads to an extension of π-orbitals, thus increases $\pi-\pi$ overlapping of neighbouring discotic cores along the

[a] A. Gowda, L. Jacob, Prof. S. Kumar
     Soft Condensed Matter Group, Raman Research Institute, C.V. Raman
     Avenue, Sadashivanagar, Bangalore − 560 080, India
     E-mail: skumar@rri.res.in
[b] Dr. D. P. Singh, Prof. R. Douali
     Unité de Dynamique et Structure des Matériaux Moléculaires (UDSMM),
     Université du Littoral Côte d'Opale, Calais − 62228, France
     Tel.: +91 80 23610122
     Fax: +91 80 23610492

columnar direction which enhances the charge carrier mobility and overwhelming semiconducting properties of discotic liquid crystals for device applications.[40–44] Therefore, the design of appropriate functionalised π-conjugation or substitution of DLCs materials may finds an immense interest for electronic devices. With this idea, we have designed and synthesised new extended π-conjugated phenazine fused triphenylene DLCs. We have also examined the charge transport properties in these materials.

Extension of triphenylene ring is relied upon to demonstrate significant changes on liquid crystalline properties along with their electronic properties. Supramolecular macrocyclic compounds are foreseen to exhibit columnar mesomorphic phases over a broad temperature range and high charge carrier mobilities.[40–51] Many approaches have been applied to enlarge the triphenylene discotic core to produce phenanthrophenazine,[52,53] hexabenzotriphenylene,[54] triphenylenophthalocyanine,[55] etc., derivatives. In a single component retaining phenazine and triphenylene cores may result in the synthesis of novel heterocyclic discotic compounds with their interesting physical and biological properties. Phenazine based materials have many advantages in the field of biological sciences such as antibacterial, insecticidal properties and organic dye components.[56-58] Presence of charge generating, transporting, polar and coloured nature of phenazine heterocyclic core along with the mesomorphic character of triphenylene derivatives can shows supramolecular framework system suitable for molecular electronic device applications. We have previously reported the synthesis and mesomorphic investigation of phenanthro[a]phenazine and phenanthro[b]phenazine based extended triphenylene DLCs obtained by the condensation of 1,2-phenylenediamine with triphenylene-1,2-diquinone derivatives.[52,53] We have also extended the work to report heterocyclic imidazole ring fused TP core that exhibits columnar mesophase over broad temperature range.[59] Yang and co-workers have prepared DLCs based on the triphenylene-bodipy dyads and investigated their photophysical properties. These mesogens exhibited strong fluorescence properties along with a high quantum yields in solution and weak fluorescence in film.[60] They have also reported triphenylene-perylene-triphenylene discotic triads along with bay substituents, which exhibit Col_h phase over a broad range of temperature and photophysical properties.[61] Similarly, Wang et al. reported the donor-acceptor dyads having triphenylene (donor)- perylene monoimide dihexyl ester (acceptor) connected through ethynylphenyl bridges which exhibit broad Col_h phase. These extended π–conjugation in aforementioned compound results an intramolecular photo-induced electronic charge transfer between the donor and acceptor units.[62] Recently, electron rich character of triphenylene twin linking through electron deficient nature of pyrazine ring that represents a donor-acceptor-donor framework like extended π−conjugation with wide range mesomorphic properties is reported by Cammidge et al.[63]

In this article, we report the design and synthesis of novel extended triphenylene based phenazine heterocyclic discotic liquid crystals containing alkanethiols and alkoxy chains. All the compounds show a wide range of stable hexagonal columnar phase. We envisioned that, the incorporation of phenazine moiety enhances π-electron conjugation and induces a wide mesophase along with high charge carrier properties. We discuss the synthesis, liquid crystalline characterization, photophysical properties and charge carrier mobility of extended triphenylene heterocyclic discotic compounds. Molecular structure of all the novel compounds was characterized using the spectral techniques and elemental analysis. The liquid crystalline properties of all the compounds were investigated with the help of polarized optical microscope (POM), differential scanning calorimetry (DSC) and X-ray diffraction (XRD) studies. The charge carrier mobility was measured by time of flight method.

2. Results and Discussion

2.1. Synthesis and characterization

We designed and synthesized the extended triphenylene fused mesogenic derivatives as shown in Scheme 1. The monohy-
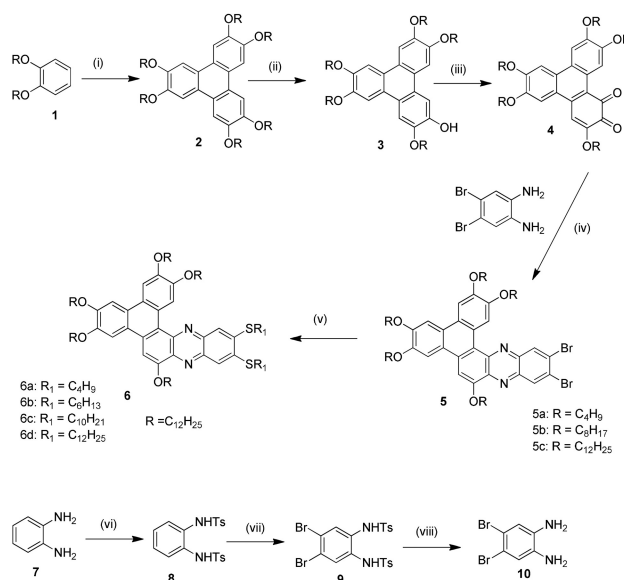
Scheme 1. (i) FeCl₃, CH₂Cl₂, r.t, 30 min; (ii) catechol boron bromide, CH₂Cl₂, r.t, 24 h; (iii) CAN, CH₃CN, r.t, 30 min; (iv) CH₃COOH: toluene (7:3), reflux, 6 h; (v) alkanethiol, Cs₂CO₃, DMAC, reflux, 24 h; (vi) p-TosCl, pyridine, r.t, 24 h; (vii) Br₂, NaOAc, acetic acid, 110 °C, 3 h; (viii) Con. H₂SO₄, 110 °C, 15 min.

droxytriphenylene **3** was synthesised following reported procedure.[64] Oxidation of the 2-hydroxy-3,6,7,10,11-pentakis(alkyloxy)triphenylene **3** with ceric ammonium nitrate (CAN) gives 3,6,7,10,11-pentakis(alkyloxy)triphenylene-1,2-diones **4**.[65] The intermediate 4,5-dibromobenzene-1,2-diamine compound was synthesized following a reported procedure[66] and it was condensed with triphenylene-1,2-diquinone **4** in presence of glacial acetic acid in toluene (7:3) under reflux condition to afford intermediate 9,10-dibromo-2,3,6,14,15-pentaalkoxyphenanthro[9,10-a]phenazine compounds (**5 a-5 c**). Further, reac-

tion of alkanethiols with intermediate mesogenic compound **5c** in presence of cesium carbonate under reflux condition produces the desired extended phenazine based triphenylene mesogenic derivatives **6a-6d**. All the intermediates and final compounds were purified by column chromatography, followed by recrystallization with appropriate solvent. The molecular structure of the compounds was characterized by ^{1}H and ^{13}C NMR spectroscopy, IR and elemental analysis.

2.2. Thermal properties

Thermotropic liquid crystalline properties of all the intermediate and final triphenylene based phenazine derivatives (**5a–5c** & **6a–6d**) are summarized in Table 1. The phase transition temperature (peak temperature in °C) and associated enthalpy (ΔH in kJ mol^{-1}) values obtained from the heating and subsequent cooling cycles of respective mesogens were determined by DSC at the scan rate of 10 °C min^{-1} under nitrogen atmosphere. The columnar textures of all the mesogens, observed using POM under crossed polarizers, display the characteristic of hexagonal columnar mesophase as shown in Figure 1.

The compound **5a** exclusively shows enantiotropic columnar phase (ESI, Figure S1). The peak temperature at 154.4 °C is due to crystalline-columnar phase transition with the enthalpy of phase transition (ΔH) of 32.42 kJ mol^{-1}, whereas the peak temperature at 315.3 °C with lower enthalpy value ($\Delta H =$ 11.21 kJ mol^{-1}) corresponds to Col$_h$ to isotropic phase transition. On slow cooling under POM, the microscopic observation of dendritic textures revealed the formation of hexagonal columnar mesophase at 312.9 °C. The crystallization was confirmed by the moderate appearance of small needle like domains into liquid crystal texture upon cooling to room temperature. As a representative example, polarized optical micrograph of compound **5a** obtained on cooling from the isotropic liquid at about 245 °C is shown in Figure 1a. Similarly, compounds **5b** and **5c** exhibit Cr to Col$_h$ phase at 94.8 °C ($\Delta H =$ 40.65 kJ mol^{-1}) and 81.3 °C ($\Delta H =$ 48.90 kJ mol^{-1}), respectively and Col$_h$ to isotropic liquid at 265.4 °C ($\Delta H =$ 8.46 kJ mol^{-1}) and 232 °C ($\Delta H =$ 7.90 kJ mol^{-1}) respectively (ESI, Figure S2). A representative DSC thermogram of intermediate compound **5c** is shown in Figure 2. Under POM, compound **5b** showed appearance of columnar texture at 263 °C, on cooling from isotropic phase. On the other hand, compound **5c** show a similar textural transition during the cooling from isotropic phase (232 °C) to room temperature.

Similar trend of enantiotropic phase transition is also observed for the final mesogenic derivatives (**6a-6d**). The compounds **6a** and **6b** show two endothermic peak transition temperatures from Cr to Col$_h$ at 55.1 °C ($\Delta H =$ 36.60 kJ mol^{-1}) and 45.7 °C ($\Delta H =$ 47.36 kJ mol^{-1}), respectively and Col$_h$ phase

Table 1. Phase transition temperature (peak in DSC °C) and enthalpies (kJ mol^{-1}, in parentheses) of all the mesogens **5a–5c** and **6a–6d** (on heating and cooling cycle). Cr = crystalline phase; Col$_h$ = hexagonal columnar phase; I = isotropic phase.

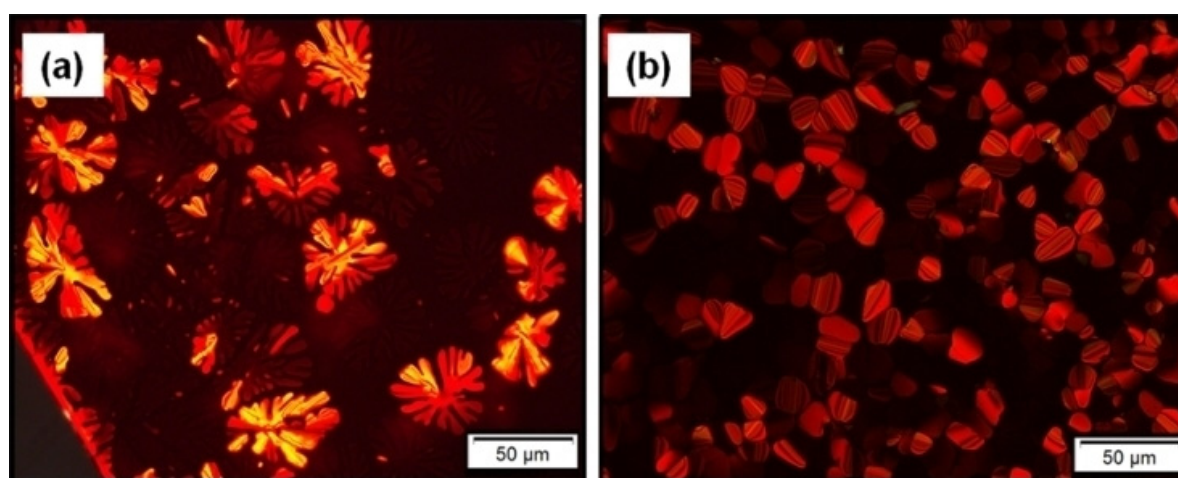| Compound	Phase transition peak temperature (°C); (ΔH, [kJ mol^{-1}]) second heating scan	second cooling scan
5a	Cr 154.4 [32.42] Col$_h$ 315.3 [11.21] I	I 312.9 [-11.61] Col$_h$ 55.2 [-18.10] Cr
5b	Cr 94.8 [40.65] Col$_h$ 265.4 [8.46] I	I 263 [-8.16] Col$_h$ 13.5 [-31.88] Cr
5c	Cr 81.3 [48.90] Col$_h$ 232 [7.90] I	I 228.9 [-7.62] Col$_h$ 17.2 [-51.58] Cr
6a	Cr 55.1 [36.60] Col$_h$ 172 [6.49] I	I 170.3 [-6.24] Col$_h$ 17.4 [-38.83] Cr
6b	Cr 45.7 [47.36] Col$_h$ 176.4 [6.66] I	I 174.7 [-6.17] Col$_h$ 19 [-45.49] Cr
6c	Cr$_1$ 44.2 [10.95] Cr$_2$ 73 [20.16] Col$_h$ 167.1 [5.38] I	I 163.2 [-5.66] Col$_h$ 23.6 [-38.39] Cr
6d	Cr$_1$ 34.5 [6.11] Cr$_2$ 74.1 [25.83] Col$_h$ 165.1 [6.72] I	I 163.5 [-6.52] Col$_h$ 35.7 [-36.04] Cr

Figure 1. Polarized optical micrographs taken in hexagonal columnar phase. (a) Compound **5a** at 245 °C, viewed at 200 × magnifications. (b) Compound **6d** at 110 °C on cooling from isotropic liquid, viewed at 200 × magnifications.
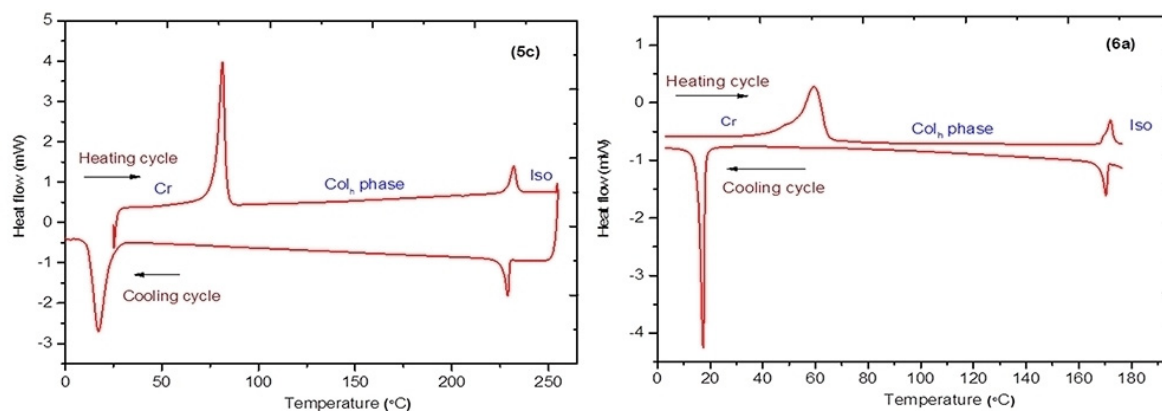
Figure 2. DSC thermogram of **5 c** and **6 a** on heating and cooling cycles (scan rate 10 °C min⁻¹).
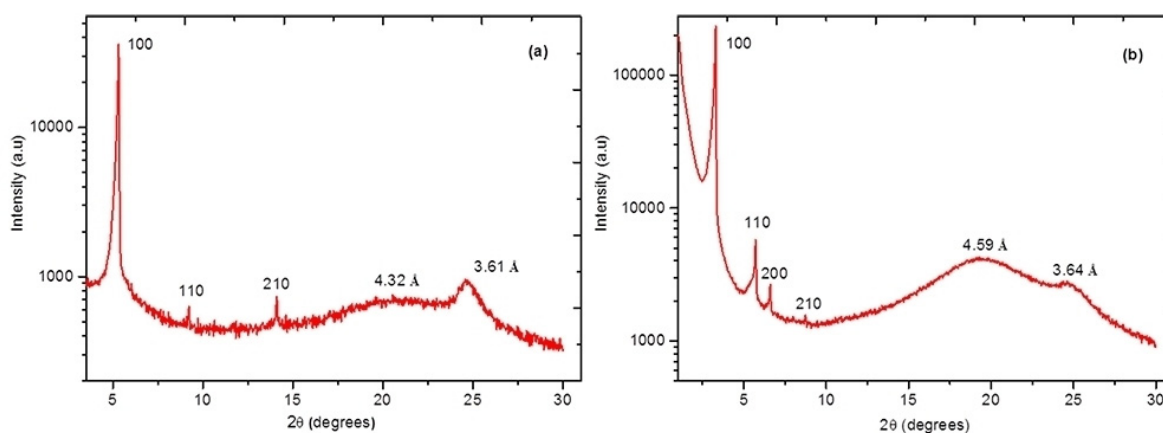

Figure 3. The intensity profile of the X-ray pattern exhibited by (a) **5 a** at 175 °C and (b) **6 d** at 100 °C respectively.

to isotropic phase at 172 °C ($\Delta H = 6.49$ kJ mol⁻¹) (Figure 2) and 176.4 °C ($\Delta H = 6.66$ kJ mol⁻¹) (ESI, Figure S3) respectively. On cooling under POM, compound **6 a** showed the appearance of columnar phase at 170.3 °C which transferred to crystalline phase at 17.4 °C. Representative DSC thermogram of **6 a** is shown in Figure 2. On the other hand, compound **6 b** observed under the POM exhibit mesophase at 174.7 °C and retain Col$_h$ phase upto 19 °C (on cooling). Upon heating and cooling scans, compound **6 c** under goes through crystal-crystal transition at 44.2 °C ($\Delta H = 10.95$ kJ mol⁻¹) and melt to Col$_h$ phase at 73 °C ($\Delta H = 20.16$ kJ mol⁻¹) and become isotropic liquid at 167.1 °C ($\Delta H = 5.38$ kJ mol⁻¹) (ESI, Figure S4). Under POM, compound **6 c** showed the formation of columnar phase texture at 163.2 °C and transferred to crystalline phase at 23.6 °C (on cooling). Similarly, on heating compound **6 d** display crystal-crystal transition at 34.5 °C ($\Delta H = 6.11$ kJ mol⁻¹) and become melting to Col$_h$ phase at 74.1 °C with enthalpy change ($\Delta H = 25.83$ kJ mol⁻¹), which goes to isotropic phase at 165.1 °C ($\Delta H = 6.72$ kJ mol⁻¹) (ESI, Figure S5). Compound **6 d**, on slow cooling form isotropic liquid exhibit typical texture of Col$_h$ phase at 163.5 °C as shown in Figure 1b, viewed at 200 × magnifications. POM and DSC studies reveal the presence of mesophase structure,

while self-assembly of hexagonal columnar phase has been investigated by X-ray diffraction studies. It is noticed that the extended phenazine core with flexible alkanethiol substituted derivatives (**6 a–6 d**) exhibit a lower isotropic temperature in comparison to intermediate dibrominated phenazine compounds (**5 a−5 c**) owing to the more number of flexible alkyl chains surrounded around the discotic core.

2.3. X-ray diffraction studies

In order to understand the mesophase structure along with the supramolecular self-assembly of all the novel mesogens, X-ray diffraction experiments were performed using liquid crystalline samples filled in Lindemann capillaries. X-ray diffraction patterns recorded for all the mesogens (**5 a-5 c** and **6 a-6 d**) in the columnar mesophase on both heating and cooling scans as shown in Table 2 and Figure 3. All the mesogenic compounds **5 a-5 c** and **6 a-6 d** showed increasing order of diffraction angle, the *d*-spacing's of the first reflection (lowest angle and highest intensity) to the second one are in the ratio of $1:1/\sqrt{3}:1/2:1/\sqrt{7}$. These values corresponding to those expected from two-dimensional hexagonal lattice and relatively broad peak in the

Table 2. X-ray data of all the mesogens (5a-5c & 6a-6d).								
Compound/ Temperature (°C)	2θ (degrees)	d-spacing's, observed (calculated) Å	Phase/ lattice constant	Col_h parameter	Miller indices	Alkyl- chain length (Å)	Core-core separation (Å)	Intercolumnar distance (Å)
5a/175	5.30	16.65 (16.64)	Col_h $a = 19.22$	1	100	4.32	3.61	19.22
	9.21	9.59 (9.60)		$1/\sqrt{3}$	110			
	14.09	6.27 (6.29)		$1/\sqrt{7}$	210			
5b/200	3.70	20.52 (20.51)	Col_h $a = 23.69$	1	100	4.51	3.65	23.69
	7.42	11.90 (11.84)		$1/\sqrt{3}$	110			
	11.39	7.75 (7.75)		$1/\sqrt{7}$	210			
5c/140	3.72	23.69 (23.68)	Col_h $a = 27.35$	1	100	4.62	3.66	27.35
	6.43	13.75 (13.67)		$1/\sqrt{3}$	110			
6a/100	3.59	24.58 (24.57)	Col_h $a = 28.38$	1	100	4.50	3.55	28.38
	6.22	14.19 (14.18)		$1/\sqrt{3}$	110			
	7.19	12.28 (12.28)		1/2	200			
6b/75	3.51	25.14 (25.13)	Col_h $a = 29.02$	1	100	4.62	3.56	29.03
	6.08	14.52 (14.50)		$1/\sqrt{3}$	110			
	7.03	12.56 (12.56)		1/2	200			
6c/130	3.36	26.27 (26.26)	Col_h $a = 30.33$	1	100	4.57	3.60	30.33
	5.72	15.46 (15.16)		$1/\sqrt{3}$	110			
	6.58	13.41 (13.13)		1/2	200			
6d/100	3.30	26.74 (26.73)	Col_h $a = 30.87$	1	100	4.59	3.64	30.87
	5.72	15.37 (15.42)		$1/\sqrt{3}$	110			
	6.61	13.35 (13.36)		1/2	200			
	8.74	10.10 (10.10)		$1/\sqrt{7}$	210			

wide angle regime corresponding to the liquid like packing of the molten aliphatic chains. The distance between neighbouring columns was calculated by using the relation $a = d_{10}/(\cos30°)$, where d_{10} is the spacing of highest intensity peak in the small angle region (Table 2). A representative and typical XRD pattern obtained for compound 5a and 6d on heating scan is shown in Figure 3. The XRD pattern of compound 5a at 175 °C during heating in columnar phase is shown in Figure 3a. In the small angle region three peaks were observed, one very strong and other two weak peaks of d- spacing $d_1 = 16.65$ Å, $d_2 = 9.59$ Å and $d_3 = 6.27$ Å values and respective lattice constant ($a = 19.22$) are in good agreement with the hexagonal columnar phase. The broad peak at wide angle region $d = 4.32$ Å corresponds to liquid like packing of molten aliphatic chains and the sharp peak at 3.61 Å corresponds to core–core distance describes ordered hexagonal columnar phase. The intercolumnar distance is found to be 19.22 Å, which is less than higher homologous derivatives 5b and 5c. Similarly, X-ray diffraction pattern obtained for alkanethiol substituted compound 6d upon heating in columnar phase at 100 °C is shown in Figure 3b. In the small angle region four prominent peaks observed, one sharp peak of d- spacing values $d_1 = 26.74$ Å and corresponding three weak peaks at $d_2 = 15.37$ Å, $d_3 = 13.35$ Å and $d_4 = 10.10$ Å, along with lattice constant $a = 30.87$, suggesting the formation of hexagonal columnar phase. The broad halo peak in the wide angle region at 4.59 Å shows liquid like arrangement of flexible chains and a weak peak at further wide angle region at 3.64 Å is analogous to the distance between cores in the columns. The intercolumnar distance for 6d is found to be 30.87 Å, which is higher than the corresponding lower homologous compounds (6a-6c) in the series. It is evident that the increase in the number of alkyl chain length, the width of the cylindrical columns framed by the discotic

molecules also increases. All the above properties obey well known supramolecular order of Col_h phase in which the disc like aromatic cores stack on top of other to form columns surrounding by the flexible molten aliphatic chains. These columns self assembled themselves in a two-dimensional hexagonal lattice. The above futures confirmed that all the mesogenic derivatives (5a−5c & 6a−6d) are self-assembled in the hexagonal columnar fashion in their liquid crystal phase.

2.4. Photophysical properties

The novel π-extended discotic mesogens (5a-5c & 6a-6d) have shown strong light absorption and photo induced light emission, as measured by UV-Vis absorption and photoluminescence studies. The UV absorption properties were studied in a very dilute solution in anhydrous chloroform solvent recorded at ambient temperature to know absorption maxima as presented in Figure 4. The details of absorption bands have been summarized in Table 3. All the mesogens display absorption bands below 600 nm. The intermediate phenazine derivatives (5a–5c) exhibit absorption at $\lambda_{max} = 257$-473 nm and molar absorption coefficient (ε) 1.34-3.94 L mol^{-1} cm^{-1}, which corresponds to n→π* and π→π* electronic transitions as shown in Figure 4a. Similarly, alkanethiol substituted phenazine derivatives show maximum absorption bands at $\lambda_{max} = 260$-469 nm and corresponding molar absorption coefficient ($\varepsilon = 2.48$-4.18 L mol^{-1} cm^{-1}), which are responsible for n→π* and π→π* electronic transitions as shown in Figure 4b. The intermediated dibrominated compounds (5a-5c) are red shifted with increased intensity to a longer wavelength ($\lambda_{max} = 473$ nm) in comparison with alkanethiol substituted phenazine derivative ($\lambda_{max} = 465$ nm). This may be attributed to extended π-conjugation along with electro-negativity effect of bromo
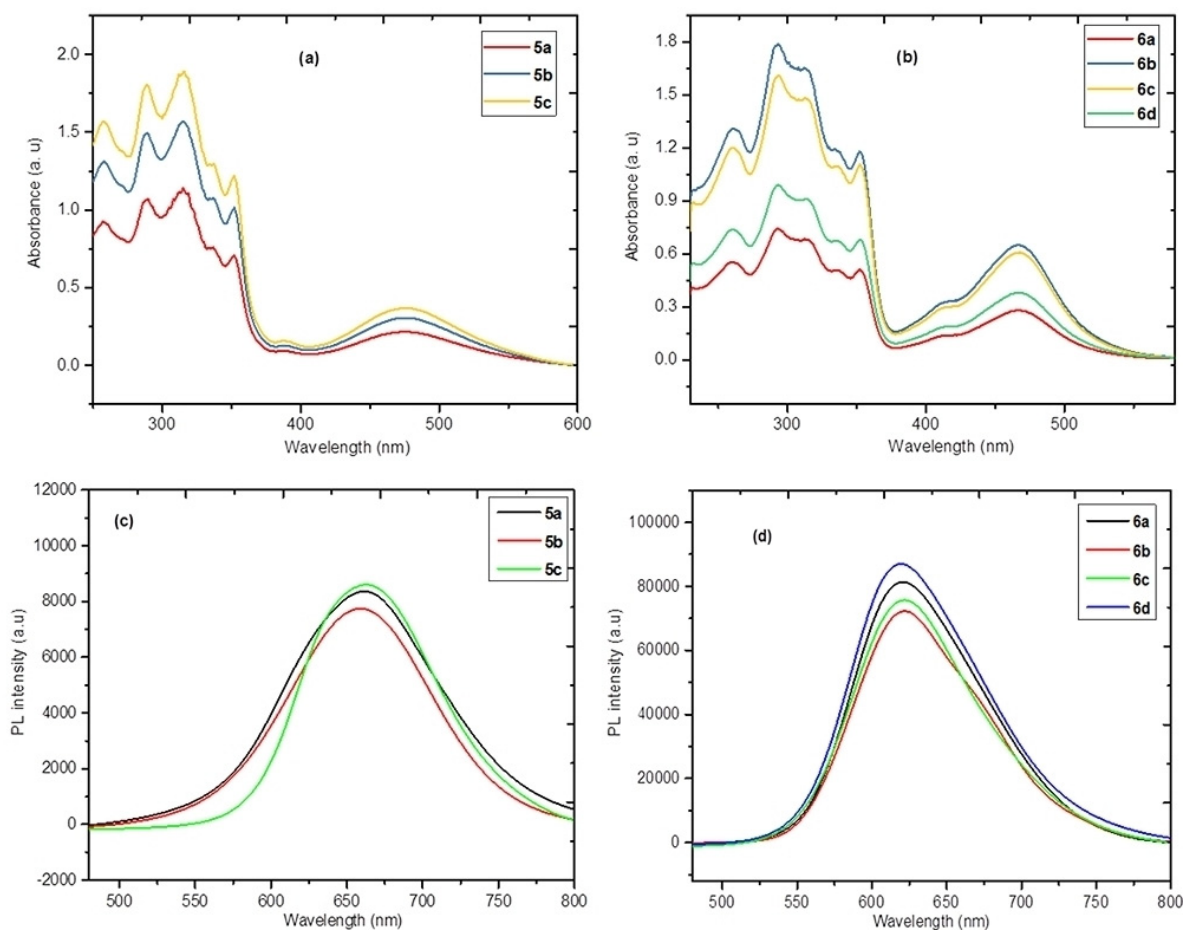
Figure 4. (a) and (b) UV-Visible absorption spectra, (c) and (d) fluorescence spectra of all the mesogens (**5a−5c & 6a−6d**).

Table 3. Photophysical properties of intermediate and final DLCs (**5a−5c & 6a−6d**) recorded in anhydrous chloroform (10^{-5} M) solution.		
Compound	Absorption, λ_{abs}/nm ($\varepsilon/10^7$ L mol^{-1} cm^{-1})	Emission,λ_{em}/ nm
5a	257 (0.72), 290 (0.82), 314 (0.88), 352 (0.99), 476 (1.34)	661
5b	258 (1.38), 289 (1.55), 315 (1.69), 352 (1.89), 476 (2.55)	659
5c	258 (2.13), 289 (2.39), 316 (2.62), 352 (2.91), 476 (3.94)	663
6a	260 (2.32), 293 (2.61), 352 (3.14), 469 (4.18)	622
6b	261 (1.38), 292 (1.54), 352 (1.86), 468 (2.48)	621
6c	261 (1.54), 294 (1.73), 352 (2.08), 468 (2.76)	622
6d	260 (2.04), 293 (2.30), 352 (2.77), 469 (3.69)	620

functional groups present in the heteroaromatic phenazine ring on molecular structure of discotic mesogen. In general, intensity of light absorption eventually relies upon the number of molecules that absorb light of a given wavelength. Extension of π- conjugation frame work in the novel mesogens (**5a−5c & 6a−6d**) causes bathochromic shift (longer wavelength) with respect to triphenylene derivatives. Similarly, photoluminescence spectra of all the mesogens (**5a−5c & 6a−6d**) were recorded using dilute solution of anhydrous chloroform solvent

at room temperature and all the compounds were excited at λ_{ex} = 460 nm as shown in Figure 4c and 4d. The intermediate dibrominated phenazine derivatives **(5a-5c),** exhibit strong emission at 659-663 nm (Table 3). Similarly, final phenazine derivatives exhibit fluorescence emission at 620-622 nm. No apparent changes were seen upon increasing the number of methylene groups in the terminal chains.

2.5. Density Functional Theory Calculations

The quantum mechanical calculations and molecular properties were determined computationally using DFT calculations. Gaussian 16 program package was employed to carry out DFT calculations at the Lee-Yang-Parr correlation functional (B3LYP) by using 6–311G (d) basis set to obtain the information related to molecular conformation and frontier molecular orbitals (FMOs) of the discotic mesogen.[67] The internal coordinates of the molecular system, which are used as an input for the Gaussian 16 computational program, were generated by the Gauss View 06 program.

The energy minimized molecular structure of representative final discotic mesogen (**6b**) is shown in Figure 5a, whereas the contours of highest occupied molecular orbital (HOMO) and
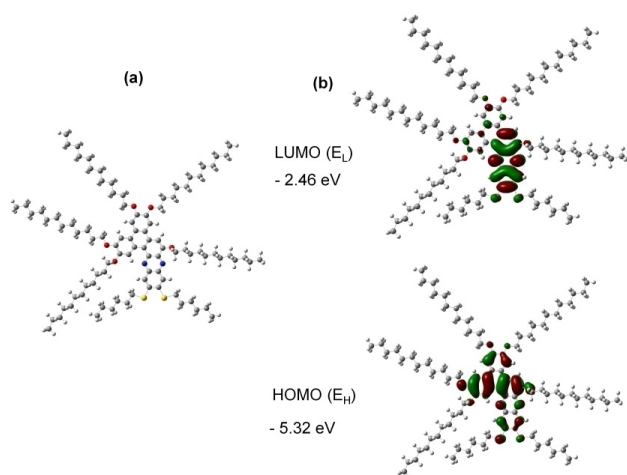
Figure 5. (a) Optimized molecular structure of compound **6 b**. (b) HOMO and LUMO frontier molecular orbital of **6 b** at the B3LYP/6.311G (d) level. E_H and E_L represents energies of highest occupied molecular orbital (HOMO) and the lowest unoccupied molecular orbital (LUMO), respectively.

lowest unoccupied molecular orbital (LUMO) is depicted in Figure 5b. The HOMO and LUMO energy levels of the compound **6 b** are at -5.32 and -2.46 eV respectively. The theoretically calculated energy gap (ΔE_{gap}) is found to be 2.86 eV. FMOs and difference in their energies provide information on the length of extended conjugation and band gap level in these novel discotic mesogens. The calculated HOMO and LUMO energy levels for the phenazine fused discotic mesogens were further illustrated to confirm the charge transfer from donor (triphenylene core) to the acceptor (phenazine core) in the excited state.[63]

2.6. Thermogravimetric analysis

Thermal stability of all novel intermediate and final discotic mesogens (**5 a−5 c** & **6 a−6 d**) was investigated by using
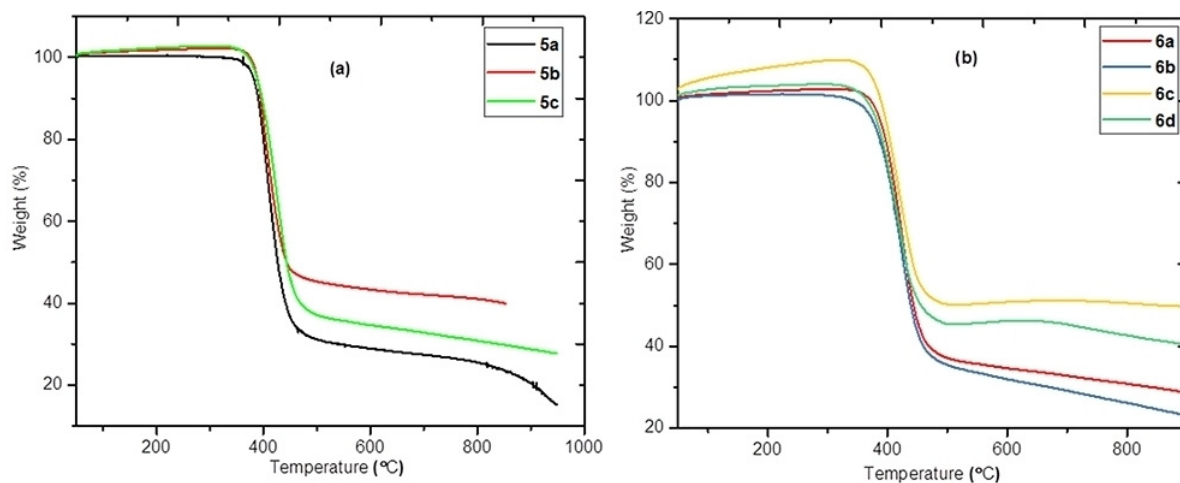
thermogravimetric analysis (TGA). All the samples were subject to heat scan of 10 °C min⁻¹ under nitrogen atmosphere as shown in Figure 6. The intermediate compounds (**5 a−5 c**) show no weight loss till 345 °C (Figure 6a) and final mesogenic compounds (**6 a−6 d**) exhibit thermal stability without weight loss until 325 °C (Figure 6b). Upon further increasing temperature, intermediate and final compounds initiated weight loss around 353 °C-375 °C (**5 a−5 c**) and 344 °C-355 °C (**6 a−6 d**), respectively. All the compounds decompose completely at 520 °C-540 °C. The thermal stability of all the compounds is much higher than their isotropic temperature. However, the thermal stability of intermediate compounds was higher than the final discotic mesogens. Hence, all the compounds are thermally stable over a broad temperature range.

3. Charge carrier mobility

We further examined the charge carrier mobility of a representative compound **6 b** using the time of flight (ToF) method. First, the LC sample was filled in the ITO cell with cell gap of 9.2 μm and then excited by Nd:YAG pulsed laser having excitation wavelength of 355 nm and 5 ns pulse width. The generation of charge carriers was examined by applying the bias of 90 to 150 V (Figure 7 and 8). The transit time (Tr) of charge carriers was obtained by the transient photocurrent curve. The induced charge displacement was recorded by a digital oscilloscope (Agilent, DSO 1012 A) connected to a current amplifier Keithley 428.

In general, the mobility (μ) is calculated using the formula; $\mu = d^2/\tau . V$, where τ is the transient time obtained by photocurrent curves, V is the applied voltage and d is the thickness of ITO cell. We adopted more precise method to calculate mobility in which, we first plotted a curve between transient time and inverse of voltage i.e. $\tau = \left(\frac{d^2}{\mu}\right)\left[\frac{1}{V}\right]$. In this relation the value of slope is equivalent to d^2/μ. Then, mobility is calculated using the formula; $\mu = d^2/slope$. The charge carrier mobility as a function of temperature is plotted in Figure 9.
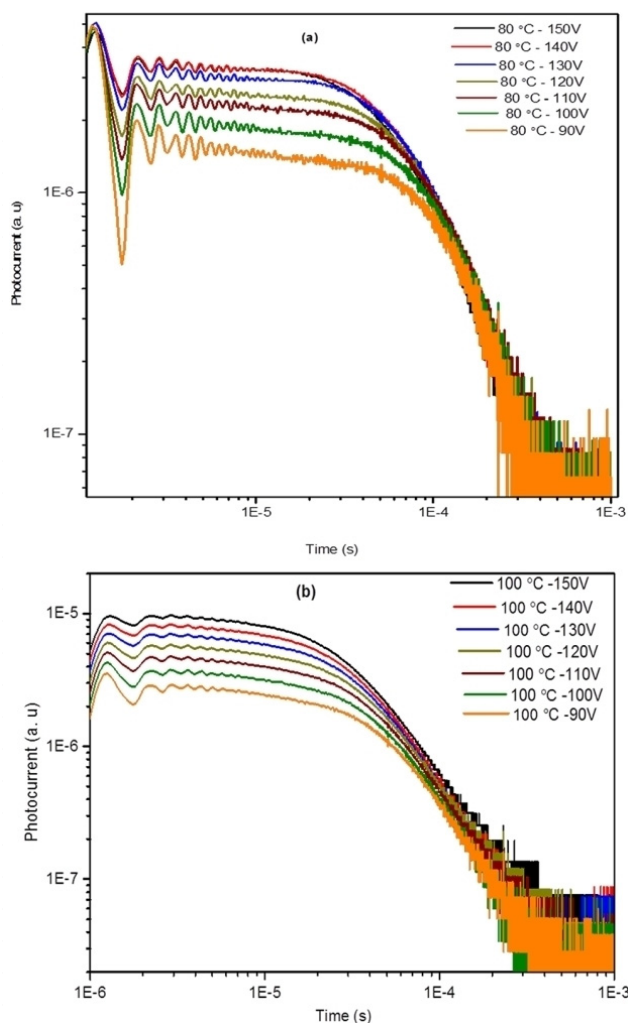

Figure 6. Thermogravimetric analysis of intermediate (**5 a−5 c**) and final discotic mesogens (**6 a−6 d**).

Figure 7. Transient photocurrent curves of compound **6 b** at (a) 80 °C and (b) 100 °C with the variation of voltage from +90 to +150 V.
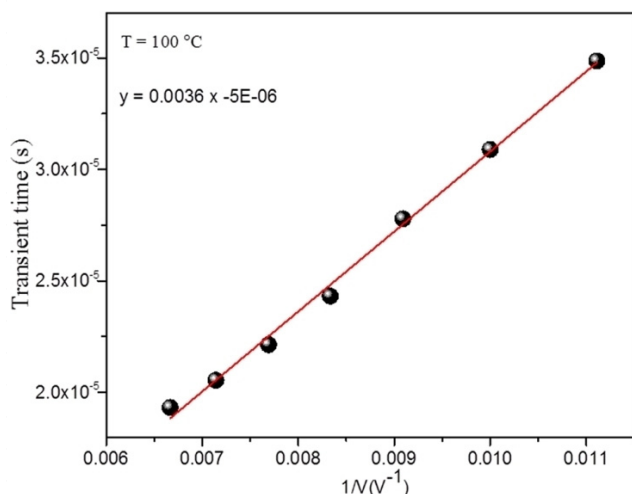

Figure 8. Transient time versus inverse of voltage curve was linearly fitted to get slope of curve.
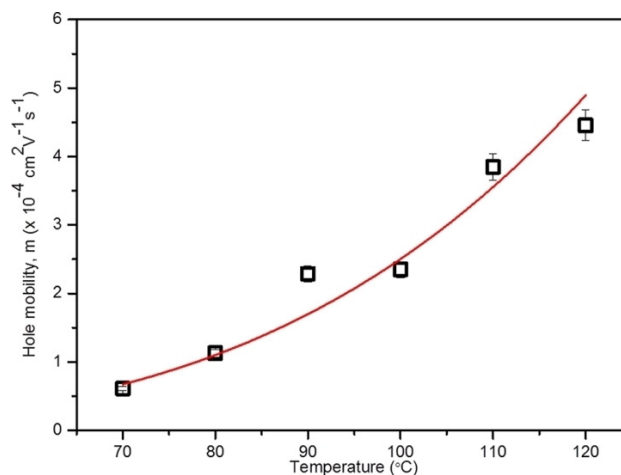

Figure 9. Hole mobility of compound **6 b** as a function of temperature. The solid line shows the fitting of experimental data by using equation 1. The values of exponent *n* and arbitrary constant *C* are found to be 3.6 and 1.09 $\times 10^{-11}$, respectively.

We observed that compound **6 b** exhibits charge transport having hole mobility in the order of 10^{-4} $cm^2V^{-1}s^{-1}$ in discotic hexagonal columnar phase which is comparable to recently reported articles.[68−71] In the present investigation, discotic material (**6 b**) exhibited *p*-type (hole) charge transport due to large triphylene core whereas charge transport due to electron associated to small phenazine was not fairly detected. Another reason for the absence of electron charge transport could be the trapping of electron by space charges or oxygen vacancies in the material. Usually, the value of charge mobility is invarient of temperature for a particular mesophase regime,[71] however, Kato *et al.* have shown the temperature dependent nature of mobility but physical mechanism behind this characteristic is not discussed.[72] We found that the charge carrier mobility increases with increasing temperature following a power law.[73]

$$\mu(T) = C.T^n \tag{1}$$

Where *C* and *n* are an arbitrary constant and an exponent, respectively.

In general, the temperature dependent mobility of single crystalline materials follows the power law[74] having negative value of exponent, *n*, varies between 0.5 to 3. For disordered mesogenic system, its value can be larger than 3. As mobility versus temperature curves are fitted well in the power law (eqn. 1), which signifies that the columnar molecular assembly is unidirectionally oriented and π-stacked columnar molecular assembly gradually grows as a function of temperature.

Current-voltage (I−V) characteristics of compound **6 b** as a function of voltage at different temperatures, ranging from 70 to 170 °C, were carried out using Keysight B2902 A Precision Source/Measure Unit (SMU). During the measurement, the temperature of ITO cell was maintained with an accuracy of ±0.1 °C using the Linkam TMS 93 hot plate. The current versus voltage (I−V) curves follow Ohmic behavior for a region of low

voltages from −10 to +10 V.[74] The charge-transport in the investigated LC system is due to the donor-acceptor mechanism of charge carriers between phenazine and triphenylene moieties. The variation of current on the temperature scale also follows the power law as shown in Figure 10, which is in good
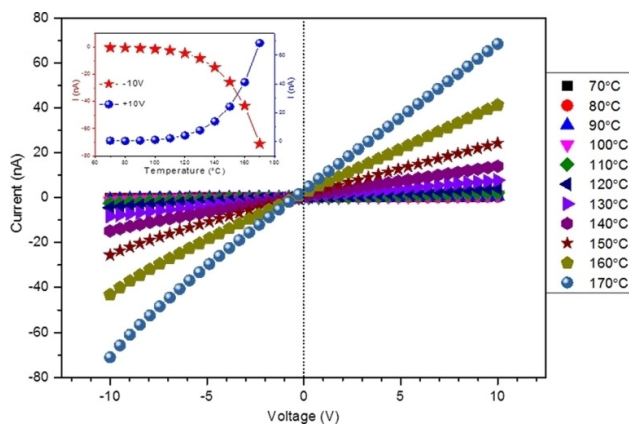

Figure 10. Current−voltage (I−V) characteristics of compound **6b** as a function of voltage for the temperature range of 70 to 170 °C. Inset shows the variation of current at ± 10 V as a function of temperature. I−V measurement was performed on 9.2 μm thick ITO cell.

agreement with the aforementioned temperature dependent behavior of mobility. This material is quite suitable for charge transportation at high temperatures and potential applications in the high temperature electronic devices and photovoltaics.

Relative permittivity of discotic mesogen **6b** as a function of temperature was evaluated at 3 kHz using a HP4284 Impedance/Gain-Phase Analyzer. In Figure 11 shows that rela-
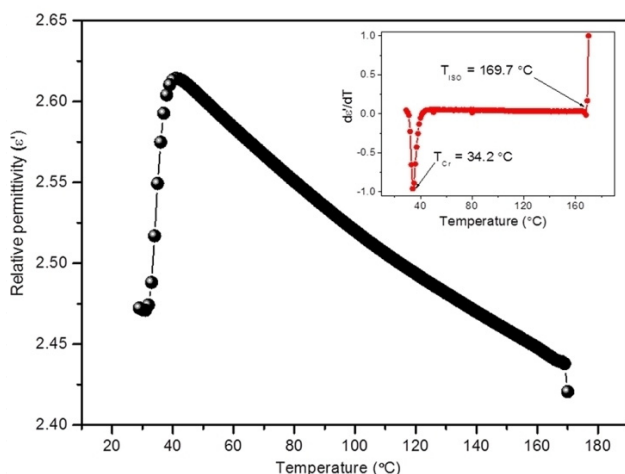

Figure 11. Relative permittivity of compound **6b** as a function of temperature evaluated at 3 kHz in cooling cycle. Inset shows the derivative of relative permittivity with respect to temperature (dε′/dT) as a function of temperature to examine the phase transition by dielectric spectroscopy. Dielectric spectroscopy was performed on 9.2 μm thick ITO cell.

tive permittivity increases with the decrease in temperature which is attributed to the thermally fluctuating π-stacked columnar molecular assembly of discotic mesogens.

4. Conclusions

The phenazine fused triphenylene discotic core containing alkanethiols and alkoxy chains have been successfully synthesised and characterised. These π−extended intermediate dibrominated phenazine derivatives and final alkanethiols containing phenazine fused TP derivatives were self organized into hexagonal columnar mesophase over a broad temperature range. The mesomorphic properties of all the compounds were further confirmed by polarized optical microscopy and differential scanning calorimetry. Hexagonal columnar structure of the liquid crystalline compounds was further confirmed by X-ray diffraction studies. All these phenazine derivatives exhibit excellent photophysical properties in anhydrous chloroform solvent. Charge carrier mobility of representative compound (**6b**) was measured by the TOF techniques, which reveals that compound (**6b**) exhibits *p*-type (hole) mobility of order 10^{-4} cm^2 V^{-1} s^{-1}. The mobility of charge carriers increases with increase in temperature following to a power law. This behavior of synthesized LC material is similar to single crystalline materials. The current-voltage characteristics follow ohmic behavior. The π-extended phenazine fused triphenylene based columnar DLCs may play a significant role in organic optoelectronic devices and solar cells applications.

Supporting Information Summary

The general methods, experimental procedure, DSC thermograms, ^1H NMR and ^{13}C NMR spectra of intermediate and final compounds have been provided in the supporting information.

Conflict of Interest

The authors declare no conflict of interest.

Keywords: charge carrier mobility · columnar phase · discotic liquid crystal · phenazine · triphenylene

[1] P. J. Collings in *Nature's Delicate Phase of Matter,* Adam Hilger, IOP Publishing Ltd, Bristol, U.K, **1990**, p. 196.
[2] T. Kato, N. Mizoshita, K. Kishimoto, *Angew. Chem. Int. Ed.* **2006**, *45*, 38−68.
[3] S. Kumar, *Chem. Soc. Rev.* **2006**, *35*, 83−109.
[4] M. T. Allen, S. Diele, K. D. M. Harris, T. Hegmann, B. M. Kariuki, D. Lose, J. A. Preece, C. Tschierske, *J. Mater. Chem.* **2001**, *11*, 302−311.
[5] H. Iino, J.-i. Hanna, *J. Opto-Electron. Rev.* **2005**, *13*, 295−302.
[6] H. K. Bisoyi, S. Kumar, *Chem. Soc. Rev.* **2010**, *39*, 264–285.

[7] S. Kumar in *Chemistry of Discotic Liquid Crystals: From Monomers to Polymers*, (Ed. V. Percec), CRC Press, Taylor & Francis Group, Boca Raton, FL, **2011**.

[8] S. Kumar in Design Concepts and Synthesis of Discotic Liquid Crystals. *In Handbook of Liquid Crystals,Vol.4* (Eds.: J. W. Goodby, P. J. Collings, T. Kato, C. Tschierske, H. F. Gleeson, P. Raynes), Wiley-VCH: Weinheim, **2014**, pp. 467–520.

[9] S. Sergeyev, W. Pisula, Y. H. Geerts, *Chem. Soc. Rev.* **2007**, *36*, 1902–1929.

[10] R. J. Bushby, K. Kawata, *Liq. Cryst.* **2011**, *38*, 1415–1426.

[11] R. J. Bushby, O. R. Lozman, *Curr. Opin. Colloid Interface Sci.* **2002**, *7*, 343−354.

[12] S. Kumar, *Isr. J. Chem.* **2012**, *52*, 820–829.

[13] S. Laschat, A. Baro, N. Steinke, F. Giesselmann, C. Hägele, G. Scalia, R. Judele, E. Kapatsina, S. Sauer, A. Schreivogel, M. Tosoni, *Angew. Chem. Int. Ed.* **2007**, *46*, 4832–4887.

[14] G. G. Nair, D. S. S. Rao, S. K. Prasad, S. Chandrasekhar, S. Kumar, *Mol. Cryst. Liq. Cryst.* **2003**, *397*, 245–252.

[15] S. Kumar, S. K. Varshney, *Angew. Chem. Int. Ed.* **2000**, *112*, 3270–3272.

[16] S. Kumar, *Pramana.* **2003**, *61*, 199–203.

[17] H. Mori, Y. Itoh, Y. Nishiura, T. Nakamura, Y. Shinagawa, *Jpn. J. Appl. Phys.* **1997**, *36*, 143–147.

[18] K. Kawata, *Chem. Rec.* **2002**, *2*, 59–80.

[19] H. Iino, J.-i. Hanna, R. J. Bushby, B. Movaghar, B. J. Whitaker, M. J. Cook, *Appl. Phys. Lett.* **2005**, *87*, 132102/1–132102/3.

[20] O. Bunk, M. M. Nielsen, T. I. Solling, A. M. van de Craats, N. Stutzmann, *J. Am. Chem. Soc.* **2003**, *125*, 2252−2258.

[21] N. Boden, R. J. Bushby, A. N. Cammidge, J. Clements, R. Luo, K. J. Donovan, *Mol. Cryst. Liq. Cryst.* **1995**, *261*, 251−257.

[22] L. Schmidt-Mende, A. Fechtenkotter, K. Mullen, E. Moons, R. H. Friend, J. D. MacKenzie, *Science.* **2001**, *293*, 1119−1122.

[23] O. I. Shklyarevskiy, P. Jonkheijm, N. Stutzmann, D. Wasserberg, H. J. Wondergem, P. C. M. Christianen, A. P. H. J. Schenning, D. M. de Leeuw, Z. Tomovic, J. Wu, k. Mullen, J. C. Maan, *J. Am. Chem. Soc.* **2005**, *127*, 16233–16237.

[24] A. Tracz, J. K. Jezka, M. D. Watson, W. Pisula, K. Müllen, T. Pakula, *J. Am. Chem. Soc.* **2003**, *125*, 1682–1683.

[25] W. Pisula, Z. Tomovic, B. El Hamaoui, M. D. Watson, T. Pakula, K. Müllen, *Adv. Funct. Mater.* **2005**, *15*, 893–904.

[26] A. M. van de Craats, J. M. Warman, A. Fechtenkötter, J. D. Brand, M. A. Harbison, K. Müllen, *Adv. Mater.* **1999**, *11*, 1469–1472.

[27] A. Bacher, I. Bleyl, C. H. Erdelen, D. Haarer, W. Paulus, H.-W. Schmidt, *Adv. Mater.* **1997**, *9*, 1031–1035.

[28] I. Seguy, P. Jolinat, P. Destruel, J. Farenc, R. Mamy, H. Bock, J. Ip, T. P. Nguyen, *J. Appl. Phys.* **2001**, *89*, 5442–5448.

[29] T. Hassheider, S. A. Benning, H.-S. Kitzerow, A.-F. Achardand, H. Bock, *Angew. Chem. Int. Ed.* **2001**, *40*, 2060–2063.

[30] A. M. van de Craats, N. Stutzmann, O. Bunk, M. M. Nielsen, M. Watson, K. Müllen, H. D. Chanzy, H. Sirringhaus, R. H. Friend, *Adv. Mater.* **2003**, *15*, 495−499.

[31] S. Cherian, C. Donley, D. Mathine, L. LaRussa, W. Xia, N. Armstrong, *J. Appl. Phys.* **2004**, *96*, 5638−5643.

[32] S. Xiao, M. Myers, Q. Miao, S. Sanaur, K. Pang, M. L. Steigerwald, C. Nuckolls, *Angew. Chem. Int. Ed.* **2005**, *44*, 7390–7394.

[33] J.-Y. Cho, B. Domercq, S. C. Jones, J. Yu, X. Zhang, Z. An, M. Bishop, S. Barlow, S. R. Marder, B. Kippelen, *J. Mater. Chem.* **2007**, *17*, 2642–2647.

[34] D. Adam, P. Schuhmacher, J. Simmerer, L. Haussling, K. Selemensmeyer, K. H. Etzbach, H. Ringsdorf, D. Haarer, *Nature.* **1994**, *371*, 141–143.

[35] M. Kumar, S. Kumar, *Polym. J.* **2017**, *49*, 85–111.

[36] J. Clements, N. Boden, T. D. Gibson, R. C. Chandler, J. N. Hulbert, E. A. Ruck-Keene, *Sens. Actuators B.* **1998**, *47*, 37−42.

[37] J. D. Wright, P. Roisin, G. P. Rigby, R. J. M. Nolte, M. J. Cook, S. C. Thorpe, *Sens. Actuators E.* **1993**, *13*, 276−280.

[38] J. Simmerer, B. Glusen, W. Paulus, A. Kettner, P. Schuhmacher, D. Adam, K.-H. Etzbach, K. Siemensmeyer, J. H. Wendorff, H. Ringsdorf, D. Haarer, *Adv. Mater.* **1996**, *8*, 815−819.

[39] D. Adam, P. Schuhmacher, J. Simmerer, L. Haussling, W. Paulus, K. Siemensmeyer, K. H. Etzbach, H. Ringsdorf, D. Haarer, *Adv. Mater.* **1995**, *7*, 276–280.

[40] R. J. Bushby, O. R. Lozman, *Curr. Opin. Solid State Matter. Sci.* **2002**, *6*, 569–578.

[41] W. Pisula, X. Feng, K. Müllen, *Chem. Mater.* **2011**, *23*, 554–567.

[42] A. Gowda, M. Kumar, S. Kumar, *Liq. Cryst.* **2017**, *44*, 1990−2017.

[43] M. Kumar, A. Gowda, S. Kumar, *Part. Part. Syst. Charact.* **2017**, *34*, 1700003/1–1700003/25.

[44] A. M. van de Craats, J. M. Warman, *Adv. Mater.* **2001**, *13*, 130−133.

[45] S. Kumar, *Liq. Cryst.* **2004**, *31*, 1037–1059.

[46] S. Kumar, *Liq. Cryst.* **2005**, *32*, 1089–1113.

[47] A. N. Cammidge, C. Chausson, H. Gopee, J. Li, D. L. Hughes, *Chem. Commun.* **2009**, 7375–7377.

[48] A. N. Cammidge, R. J. Bushby In *Handbook of Liquid Crystals, Vol. 2* (Eds.: D. Demus, J. W. Goodby, G. W. Gray, H.-W. Spiess, V. Vill), Wiley-VCH, Weinheim, **1997**, pp. 693–748.

[49] L. Zhang, H. Gopee, D. L. Hughes, A. N. Cammidge, *Chem. Commun.* **2010**, *46*, 4255–4257.

[50] L. Zhang, D. L. Hughes, A. N. Cammidge, *J. Org. Chem.* **2012**, *77*, 4288−4297.

[51] X. Kong, Z. He, Y. Zhang, L. Mu, C. Liang, B. Chen, X. Jing, A. N. Cammidge, *Org. Lett.* **2011**, *13*, 764–767.

[52] S. Kumar, M. Manickam, *Liq. Cryst.* **1999**, *26*, 1097–1099.

[53] S. Kumar, M. Manickam, *Mol. Cryst. Liq. Cryst.* **2000**, *338*, 175–179.

[54] T. Yatabe, M. A. Harbison, J. D. Brand, M. Wagner, K. Mullen, P. Samori, J. P. Rabe, *J. Mater. Chem.* **2000**, *10*, 1519–1525.

[55] A. N. Cammidge, H. Gopee, *Chem. Commun.* **2002**, 966–967.

[56] M. Krishnaiah, N. R. de Almeida, V. Udumula, Z. Song, Y. S. Chhonker, M. M. Abdelmoaty, V. A. do Nascimento, D. J. Murry, M. Conda-Sheridan, *Eur. J. Med. Chem.* **2018**, *143*, 936−947.

[57] L. S. Pierson, E. A. Pierson, *Appl. Microbiol. Biotechnol.* **2010**, *86*, 1659–1670.

[58] A. M. Shaikh, B. K. Sharma, S. Chacko, R. M. Kamble, *New J. Chem.* **2017**, *41*, 628–638.

[59] S. Kumar, S. K. Gupta, *Tetrahedron Lett.* **2011**, *52*, 5363–5367.

[60] X. Fang, H. Guo, J. Lin, F. Yang, *Tetrahedron Lett.* **2016**, *57*, 4939–4943.

[61] H. Guo, M. Zhu, Z. Wang, F. Yang, *Tetrahedron Lett.* **2016**, *57*, 4191–4195.

[62] X. Kong, H. Gong, P. Liu, W. Yao, Z. Liu, G. Wang, S. Zhang, Z. He, *New J. Chem.* **2018**, *42*, 3211–3221.

[63] W. Xiao, Z. He, S. Remiro-Buenamañana, R. J. Turner, M. Xu, X. Yang, X. Jing, A. N. Cammidge, *Org. Lett.* **2015**, *17*, 3286–3289.

[64] S. Kumar, M. Manickam, *Synthesis.* **1998**, 1119–1122.

[65] S. Kumar, M. Manickam, S. K. Varshney, D. S. S. Rao, S. K. Prasad, *J. Mater. Chem.* **2000**, *10*, 2483–2489.

[66] J. Shao, J. Chang, C. Chi, *Org. Biomol. Chem.* **2012**, *10*, 7045–7052.

[67] M. J. Frisch, G. W. Trucks, H. B. Schlegel, G. E. Scuseria, M. A. Robb, J. R. Cheeseman, G. Scalmani, V. Barone, G. A. Petersson, H. Nakatsuji, M. Caricato, X. Li, H. P. Hratchian, A. F. Izmaylov, J. Bloino, G. Zheng, J. L. Sonnenberg, M. Hada, M. Ehara, K. Toyota, R. Fukuda, J. Hasegawa, M. Ishida, T. Nakajima, Y. Honda, O. Kitao, H. Nakai, T. Vreven, J. A. Montgomery, Jr., J. E. Peralta, F. Ogliaro, M. Bearpark, J. J. Heyd, E. Brothers, K. N. Kudin, V. N. Staroverov, R. Kobayashi, J. Normand, K. Raghavachari, A. Rendell, J. C. Burant, S. S. Iyengar, J. Tomasi, M. Cossi, N. Rega, J. M. Millam, M. Klene, J. E. Knox, J. B. Cross, V. Bakken, C. Adamo, J. Jaramillo, R. Gomperts, R. E. Stratmann, O. Yazyev, A. J. Austin, R. Cammi, C. Pomelli, J. W. Ochterski, R. L. Martin, K. Morokuma, V. G. Zakrzewski, G. A. Voth, P. Salvador, J. J. Dannenberg, S. Dapprich, A. D. Daniels, O. Farkas, J. B. Foresman, J. V. Ortiz, J. Cioslowski, D. J. Fox, Gaussian 16, Gaussian, Inc., Wallingford CT, **2017**.

[68] Y. Funatsu, A. Sonoda, M. Funahashi, *J. Mater. Chem. C.* **2015**, *3*, 1982–1993.

[69] B. Feringan, P. Romero, J. L. Serrano, C. L. Folcia, J. Etxebarria, J. Ortega, R. Termine, A. Golemme, R. Gimenez, T. Sierra, *J. Am. Chem. Soc.* **2016**, *138*, 12511–12518.

[70] W. Zhang, S. Zhang, Z. Zhang, H. Yang, A. Zhang, X. Hao, J. Wang, C. Zhang, J. Pu, *J. Phys. Chem. B* **2017**, *121*, 7519–7525.

[71] H. Iino, J.-i. Hanna, D. Haarer, *Phys. Rev. B* **2005**, *72*, 193203/1– 193203/4.

[72] K. P. Gan, M. Yoshio, Y. Sugihara, T. Kato, *Chem. Sci.* **2018**, *9*, 576–585.

[73] J. Heck, J. J. Kranz, M. Elstner, *J. Chem. Theory Compt.* **2016**, *12*, 3087–3096.

[74] J. Eccher, G. C. Faria, H. Bock, H. V. Seggern, I. H. Bechtold, *ACS Appl. Mater. Interfaces.* **2013**, *5*, 11935–11943.